Available online at www.sciencedirect.com

ScienceDirect

Physics Procedia 70 (2015) 858 – 862

Physics Procedia

2015 International Congress on Ultrasonics, 2015 ICU Metz

# Fabrication of ZnO Nanowire Based Piezoelectric Generators and Related Structures

Charles Opoku[a]*, Abhishek Singh Dahiya[a], Christopher Oshman[b], Frederic Cayrel[a], Guylaine Poulin-Vittrant[b], Daniel Alquier[a], Nicolas Camara[a]

[a]Université François Rabelais de Tours, CNRS, GREMAN UMR 7347, 16 rue Pierre et Marie Curie, 37071 TOURS Cedex2, France.
[b]Université François Rabelais de Tours, INSA-CVL, CNRS, GREMAN UMR 7347, 3 rue de la Chocolaterie, CS 23410, 41034 BLOIS Cedex, France.

**Abstract**

Using vertically grown hydrothermal ZnO nanowires, we demonstrate the assembly of fully functional piezoelectric energy harvesters on plastics substrates. A seedless hydrothermal process is employed for the growth of single crystalline vertically orientated ZnO NWs at around 100°C. Flexible NG are assembled using ~7µm thick PDMS polymer matrix on a 3x3cm substrate. A representative device with an active area of 4cm$^2$ is characterised revealing average output voltage generation of ~22mV (±1.2) and -32mV (±0.16) in the positive and negative cycles after 3-4mm periodic deflection at 20Hz. A power density of ~288nW/cm$^3$ is estimated for the device. It is envisaged that such energy scavengers may find potential applications targeting self-powered systems, sensors and on-body charging of electronics.


Peer-review under responsibility of the Scientific Committee of ICU 2015

*Keywords:* Piezoelectric; Nanogenerators; Zinc oxide; Nanowires

## 1.0 Introduction

Energy harvesters can be practically assembled using low-cost solution assembly methods to siphon and convert ambient mechanical energy into electricity [Zhu et al (2012), Beeby et al (2006), Lee et al (2013) Chen et al (2010)].The appeal of this technology can be further enhanced with solution derived piezoelectric nanostructures, that can be

* Dr Charles Opoku. Tel.: +33247424000 ext. 4826.
*E-mail address:* Charles.opoku@univ-tours.fr


Peer-review under responsibility of the Scientific Committee of ICU 2015
doi:10.1016/j.phpro.2015.08.176

grown at low temperatures and over large-area substrates [Briscoe et al (2013)]. ZnO nanowires have emerged as potential materials for this technology due to its unique properties, offering inorganic piezoelectric material performance (e.g. PZT) with organic (e.g. PVDF) processability [Briscoe et al (2013), Park et al (2014)], Lee et al (2012)]. These features have led to demonstrations various of energy scavengers called "piezoelectric nanogeneratorS" (NG). NGs can be categorised by two main configurations, called the "vertically integrated" and "laterally integrated" (VING and LING, respectively). Due to the relative ease of fabrication, the former is by far and away the most developed [Zhu et al (2012), Lee et al (2013), Briscoe et al (2013), Hinchet et al (2014)]. Array of vertically orientated ZnO NW on conductive substrates are initially encased in a non-conductive polymer to form a composite. Metallic layers are deposited on the surface of this composite to complete device fabrication [Briscoe et al (2013)]. In operation, application of a force induces in an apparent potential gradient across the NG thickness, as a result of the piezoelectric effect. In turn, this potential can be used to drive charges in an external circuit. Using this design, demonstrations of truly impressive electrical outputs from ZnO NGs encased in polymers like polymethyl methacrylate (PMMA) polymer [Zhu et al (2012), Hu, Y., et al (2012)]. Reports also exist on ZnO NW NGs employing other polymers like p-type PEDOT:PSS and thick Polydimethylsiloxane (PDMS) polymers [Briscoe et al (2013), Lin et al (2013)]. Herein, we demonstrate the synthesis of ZnO NW and their successful integration into fully flexible piezoelectric nanogenerator on plastic. The ZnO NWs functioned as the primary piezoelectric elements encased in ~7µm thick PDMS as the polymer matrix. Such thin conformal matrix layers atop NWs were obtained by diluting PDMS mixtures with toluene. We show that periodically deflecting the NGs resulted in a corresponding output voltage across a 1MΩ load. Extraction on key parameters revealed peak output voltages of ~22mV (±1.2) and -32mV (±0.16) in the positive and negative cycles, respectively. The total output power, normalised to the volume was estimated to be ~288nW/cm$^3$.

## 2.0 ZnO nanowire Synthesis

The ZnO nanowires were synthesized at around 100$^o$C on Au/Ti coated Polyethylene naphthalate substrates (PEN, DuPont) by the hydrothermal reaction, as in reported data elsewhere [Tian et al (2011), Xu et al (2009)]. The reaction nutrients zinc nitrate hexahydrate ($Zn(NO_3)_2{\cdot}6H_2O$) and Hexamethylenetetramine ($C_6H_{12}N_4$) at ~100mmol and 10mmol ammonium hydroxide ($NH_4{\cdot}4OH$, 30% wt%, reagent grade, Sigma Aldrich). Substrates were immersed face down in a Teflon lined stainless steel Autoclave reactor and placed in a preheated convection for the reaction to take place (~12-15hrs). After synthesis, substrates were retrieved and rinsed thoroughly in DI-water and then baked on a hotplate for up to 10 min (100$^o$C).

### *2.1 ZnO Nanowire characterisation*

The ZnO NWs were characterised by scanning electron and transmission electron microscopy (SEM and TEM, respectively). Fig. 1, shows the SEM images of the ZnO NWs. From these images, we obtained high density ZnO NWs with hexagonal morphologies at the top surface. Fig. 1b shows that NWs exhibited high degree of structural orientation. Assessment of several SEM images revealed the average diameter, length and density to be around ~115nm ±64, ~0.97µm ±0.34, ~74.5µm ±6.5, respectively. Such excellent characteristics are essential for realising fully functional ZnO NW based NGs. Fig. 2 shows the high resolution TEM (HRTEM) data for a representative ZnO NW grown by the present method. From this data, it can be seen that highly crystalline ZnO NW material were obtained. The inset show the selected area electron diffraction pattern, where the growth direction was confirmed to be that of [0001] wurtzite ZnO.

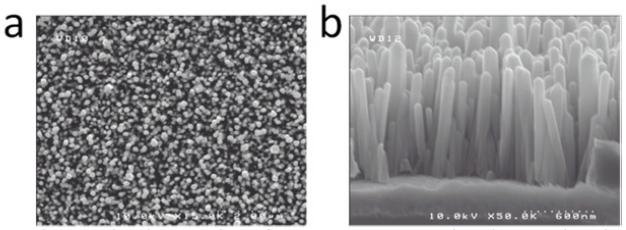


Figure 1. Scanning Electron microscope images showing top view of as-grown ZnO nanowires. b) Scanning electron microscope image showing cross-sectional profile of the ZnO nanowires. c-d) Side view of the ZnO NWs are various magnifications.

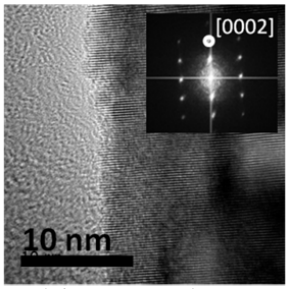


Figure 2. High resolution transmission electron micrograph for a representative ZnO nanowire. Inset shows the Fast Fourier Transform of the image.

## 2.0 Nanogenerator Assembly and Proposed Working Principle

Using the as-grown ZnO NWs on Au/Ti-PEN substrates, fully functional NGs were assembled. The fabrication steps undertaken for NG assembly can be schematically visualised from Fig. 3a-d. A PDMS mixture (1:7:3 of cross linker, PDMS base and toluene) was first dispensed onto substrates containing the vertical ZnO NWs. A degassing step under low vacuum (~1-2hrs) was performed, followed by spin coating at ~3000rpm (~60s). This was followed by baked at around 100$^{o}$C to cross-link deposited PDMS. Next, approximately 400nm/100nm thick Al/Ti layers were evaporated on the top surface of ZnO NW-PDMS matrix to define the working area of devices. To complete device fabrication, copper wires were bonded to the top and bottom conductive surfaces conductive using silver paste.

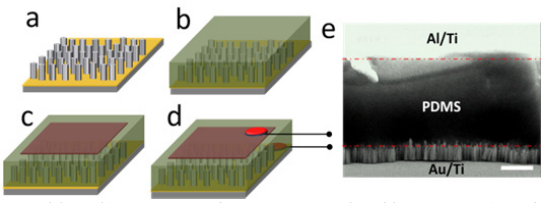


Figure 3. Process flow steps for NG assembly. a-b) ZnO nanowires are encapsulated by PDMS. c) Active area defined by evaporating Al/Ti (~400/100nm) on top of ZnO-polymer surface. d) Bonding of copper wires to the top and bottom surfaces. e) Cross-sectional SEM image of a fabricated NG.

The NGs were also encapsulated in thick PDMS to minimise excessive degradation during testing. Previous studies have demonstrated functional NGs with thick PDMS (~200μm) as both substrate and separating layer between NW base and bottom electrode [Lin et al (2013)]. Surprisingly little data exists on its use as the infiltration matrix in ZnO NW based NGs. Fig. 3e shows the SEM image of a cleaved NG with diluted PDMS matrix. From this image, it can be seen that ZnO NWs were effectively encapsulated by the polymer. The PDMS layer above the NWs was around ~7μm (±0.5). Notably, the matrix layer of 7μm above ZnO NW tops is significantly lower than that used by [Lin et al

(2013)], where a maximum power output of ~5.3mW/cm$^3$ was reported.

## 3. Nanogenerator Working Principle

The process of converting mechanical energy into electrical energy using NGs is well documented [Hinchet et al (2014), Wang (2001)]. In this work, we make the assumptions that: (1) due to the relative thickness of both substrate and PDMS-top electrode, inwards bending of the device induces a compressive strain along the vertical ZnO NWs [Lee et al (2014)]. This strain displaces ionic constituents inside ZnO NWs, resulting in the creation of piezoelectric potential in the ZnO NW filaments. (2) The PDMS layer separating the top electrode from NW tops can be regarded as a capacitor [Hinchet et al (2014)]. (3) Assuming positive net charges atop ZnO NWs, with the corresponding negative charges on the top electrode. Finally, (4) the capacitance associated with the ZnO-Au interface ensures that the bottom electrode is net positive. With these conditions, periodically bending and releasing the NG will generate an alternating voltage that can be detected across a resistive load. The magnitude of this voltage will depend on the rate deformation due to losses [Briscoe et al (2013)]. The PDMS thickness atop NWs is also expected influence the density of charge ($Q \approx \varepsilon E$) that can be collected.

## 4.0 Nanogenerator Test

The NGs in this work were characterised on a custom built test-bench comprising of a mechanical shaker, a ridged aluminium actuator arm and a 1MΩ load. The actuator arm was attached to the reciprocating shaker platform at one end and a height adjustable screw was inserted through it on the opposite end. The screw tip was insulated by styrene-butadiene rubber to avoid excessive damage to NGs during testing. One end of the NGs were firmly fixed onto an aluminium block and the opposite end was free to be deflected (Fig. 4a).

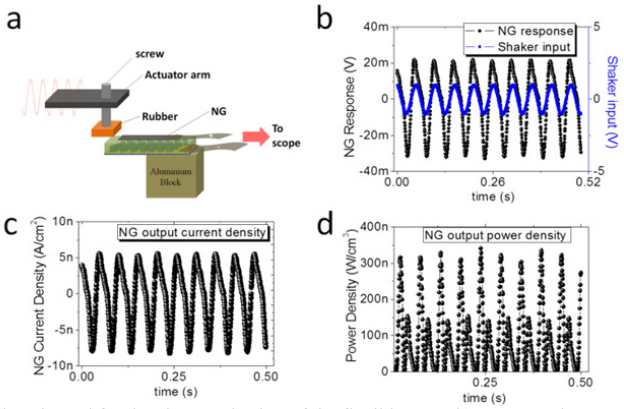


Figure 4 a) Schematic of the test bench used for the characterisation of the flexible NGs. b) Output voltage response and c) calculated output current for the same device, thanks to the 1MΩ voltage probe.

The screw tip was positioned in contact with NGs at the unclamped end during testing. Throughout the measurements, a constant deflection of the flexible NGs of 3-4mm (±0.5) was maintained. Finally, all measurements were recorded with an Agilent DSO5054A oscilloscope via a 1MΩ voltage probe. The output response of an energy harvester are generally presented in the form of output voltage V and/or current density J vs. time. Fig. 4b show the output voltage response for a representative flexible NG at constant deflection (~3-4mm) for a 20Hz actuation. From the general progression of the output response, we measure the peak voltages in the positive and negative cycles were extracted to be ~22mV (±1.2) and -32mV (± 0.16), respectively. Considering that the measured output is the voltage drop across the 1MΩ probe, the current density per cycle can estimated $J$ to around ~5.5nA/cm$^2$ (positive cycle) and 8nA/cm$^2$ (negative cycle), as shown in Fig. 4c. From the expression: $P = \frac{V^2}{R}$, where $P$ is power, $V$ is voltage drop across the resistor R, the volume normalised power density per cycle can be estimated to be around

~288nW/cm$^3$ (Fig. 4d). We note that this expression for power is only valid in an ideal case, due to stray reactance associated with the load. Although, the significance of this on the measured data is minimal at such low frequencies. Nonetheless, accuracy of the data can still be improved with sufficient compensation. Finally we are aware that this peak output power is still based on the maximum average voltage generated at a given excitation rate. The impact of losses in the present energy harvester is expect to lead to a rate dependant output as a result of high the excess free carriers in hydrothermal ZnO NWs [Hinchet et al (2014), Sohn, et al (2013)].

## 5.0 Conclusion

Functional piezoelectric nanogenerators are demonstrated using ZnO nanowire (ZnO NW) arrays on Polyethylene naphthalate (PEN) substrates. The ZnO NWs were synthesized by hydrothermal reaction on Au/Ti coated substrates in the absence of any ZnO seed layers. The fabricated NGs employed diluted Polydimethylsiloxane (PDMS) in toluene as infiltration matrix to ensure thin polymer layers atop ZnO NW. Output response of a representative NG was assessed on a custom built test bench based on a mechanical shaker. Periodically deflecting the NG resulted in a measured output voltage across a 1MΩ load connected. Extraction on key parameters revealed peak output voltages of ~22mV (±1.2) and -32mV (±0.16) in the positive and negative cycles, respectively. The total output power, normalised to the volume was estimated to be ~288nW/cm$^3$. It is hoped that enhancement in device performance can be made by reducing of the thickness of the polymer layer above NWs and/or suppressing the excess free carriers in the present hydrothermal ZnO NWs used in this work.

## Acknowledgements

This work was funded by the Region Centre CEZnO project (Convertisseur Electromécanique à base de nanofils ZnO, 2011-2014). the Authors are grateful for the supports from MEPS-Flexible (2015-2018) and ANR FLEXIBLE projects (ANR-14-CE08-0010-01). The Authors are also grateful to the Labex and GaNeX groups for collaboration.

## References

Zhu, G., et al., *Functional Electrical Stimulation by Nanogenerator with 58 V Output Voltage.* Nano Letters, 2012. **12**(6): p. 3086-3090.

Beeby, S.P., M.J. Tudor, and N.M. White, *Energy harvesting vibration sources for microsystems applications.* Measurement Science and Technology, 2006. **17**(12): p. R175.

Lee, S., et al., *Super-Flexible Nanogenerator for Energy Harvesting from Gentle Wind and as an Active Deformation Sensor.* Advanced Functional Materials, 2013. **23**(19): p. 2445-2449.

Chen, X., et al., *1.6 V Nanogenerator for Mechanical Energy Harvesting Using PZT Nanofibers.* Nano Letters, 2010. **10**(6): p. 2133-2137.

Briscoe, J., et al., *Measurement techniques for piezoelectric nanogenerators.* Energy & Environmental Science, 2013. **6**(10): p. 3035-3045.

Park, K.-I., et al., *Highly-Efficient, Flexible Piezoelectric PZT Thin Film Nanogenerator on Plastic Substrates.* Advanced Materials, 2014. **26**(16): p. 2514-2520.

Lee, M., et al., *A Hybrid Piezoelectric Structure for Wearable Nanogenerators.* Advanced Materials, 2012. **24**(13): p. 1759-1764.

Hinchet, R., et al., *Performance Optimization of Vertical Nanowire-based Piezoelectric Nanogenerators.* Advanced Functional Materials, 2014. **24**(7): p. 971-977.

Hu, Y., et al., *Replacing a Battery by a Nanogenerator with 20 V Output.* Advanced Materials, 2012. **24**(1): p. 110-114.

Lin, L., et al., *Transparent flexible nanogenerator as self-powered sensor for transportation monitoring.* Nano Energy, 2013. **2**(1): p. 75-81.

Tian, J.-H., et al., *Improved seedless hydrothermal synthesis of dense and ultralong ZnO nanowires.* Nanotechnology, 2011. **22**(24): p. 245601.

Xu, S., et al., *Optimizing and Improving the Growth Quality of ZnO Nanowire Arrays Guided by Statistical Design of Experiments.* ACS Nano, 2009. **3**(7): p. 1803-1812.

Wang, Z.L., *Piezoelectric Nanogenerators for Self-Powered Nanosensors and Nanosystems*, in *Wiley Encyclopedia of Electrical and Electronics Engineering*. 2012, John Wiley & Sons, Inc.

Lee, S., et al., *Ultrathin Nanogenerators as Self-Powered/Active Skin Sensors for Tracking Eye Ball Motion.* Advanced Functional Materials, 2014. **24**(8): p. 1163-1168.

Sohn, J.I., et al., *Engineering of efficiency limiting free carriers and an interfacial energy barrier for an enhancing piezoelectric generation.* Energy & Environmental Science, 2013. **6**(1): p. 97-104.